

Gas properties of winter lake ice in Northern Sweden: ~~Biogeochemical processes and implication~~ Implication for carbon gas release

T. Boereboom¹, M. Depoorter ^{1*}, S. Coppens¹, J-L. Tison¹

[1]{Laboratoire de Glaciologie, Université Libre de Bruxelles, Belgium}

[*]{Now at Bristol Glaciology Centre, University of Bristol, UK}

Correspondence to: T. Boereboom (thierry.boereboom@ulb.ac.be)

Abstract

This paper describes gas composition, total gas content and bubbles characteristics in winter lake ice for four adjacent lakes in a discontinuous permafrost area. Our gas mixing ratios for O₂, N₂, CO₂, and CH₄ suggest that gas exchange occurs between the bubbles and the water before entrapment in the ice. Comparison between lakes enabled us to identify 2 major “bubbling events” shown to be related to a regional drop of atmospheric pressure. Further comparison demonstrates that winter lake gas content is strongly dependent on hydrological connections: according to their closed/open status with regards to water exchange, lakes build up more or less greenhouse gases (GHG) in their water and ice cover during the winter, and release it during spring melt. These discrepancies between lakes need to be taken into account when establishing a budget for permafrost regions. Our analysis allows us to present a new classification of bubbles, according to their gas properties. Our methane emission budgets (from 6.52 10⁻⁵ to 12.7 mg CH₄ m⁻² d⁻¹ at 4 different lakes) for the three months of winter ice cover is complementary to the other budget estimates, as our approach encompasses inter- and intra-lake variability taking into account the variability of the gas distribution in the ice and between the various types of lakes.

Most available studies on boreal lakes have focused on quantifying GHG emissions from sediment by means of various systems collecting gases at the lake surface, and this mainly during the summer “open water” period. Only few of these have looked at the gas enclosed in the winter ice-cover itself. Our approach enables us to integrate, for the first time, the history of winter gas emission for this type of lakes.

1 Introduction

Lakes in subarctic environments are affected by and contribute to the current global warming. In permafrost areas, lakes are net emitters of methane and carbon dioxide, ~~two which both contribute to the~~ greenhouse gases (GHG) effect. Lakes areas in these regions represent up to 30% of land surface (e.g. Walter et al., 2008) and this ratio could increase in the coming years, as permafrost degradation supports lakes development. These lakes, embedded in recently unfrozen sediments, sustain anaerobic condition favouring methane emissions. The latter have been largely studied in recent years (e.g. review Table in Walter et al., 2010), since they are recognized as an important contributor to the greenhouse effect. Nevertheless, CH₄ emissions are still not included in Global Climate Models (GCMs) because of large uncertainties (IPCC, 2007; Koven et al. 2011).

Methane is produced ~~within lake in the~~ sediments; ~~where it as a~~ results ~~from of~~ acetate fermentation or CO₂ reduction in anaerobic ~~environments~~ conditions. ~~It~~ Methane reaches the atmosphere through the plants system, by bubbling or by diffusion through the water column. Bubbling is easily ~~identifiable-identified at on the water-lake~~ surface ~~mainly in spring and summer~~ and has been ~~mainly is largely~~ studied during ice free periods using various techniques (e.g. floating chambers, bubble traps, inverted funnel systems~~---~~). During winter periods, bubbles are enclosed in the ice, indicating that methane emission from sediment is still an active process. In peculiar situations, the emissions are so intense that they inhibit the ice formation (hotspot). The transit in the water column can induce several biochemical reactions. Methane can be oxidized to CO₂ in an oxic medium, via methanotrophic bacteria, and lakes can supply such an environment depending on their geometry and hydrology. Due to the temperature of the maximum of density of fresh water (+4°C), lakes in periglacial areas are known as dimictic i.e. presenting two periods of stratification and two overturn events~~;~~ ~~one~~ The first overturning events happen at springtime ~~during spring~~, soon after ice cover melting, and the ~~other~~ second one when the winter ~~begins~~ starts, before freeze in (Bastviken et al., 2004; Casper et al., 2000). Stratification favours the development of an anoxic layer whereas overturning causes oxygenation in the water column. Lakes are therefore mainly stratified during the winter and the ice cover will further limit atmosphere – water interactions. This closed system will result in the buildup of CO₂ and CH₄ concentrations in the water and mixing ratios in the ice. ~~During~~ At spring melt, these gases will be released to the atmosphere within a few days (Michmerhuizen et al., 1996). Methane will resituate

mainly from ice melting and bubbles emissions while carbon dioxide will release rather from gas ~~re-equilibration~~diffusion as water overturns and equilibrates with the atmosphere (Casper et al., 2000; Michmerhuizen et al., 1996; Phelps et al., 1998). Indeed, the solubility of these two gases is very different: in fresh water at 20°C pure CH₄ saturation is about 1.6 mol m⁻³ whilst the CO₂ saturation is reached at about 39 mol m⁻³. Moreover, lakes characteristics (size, depth, water circulation, hydrological system~~---~~) should also influence gas emissions, a process which has only been scarcely described.

Most studies have performed measurements on open water and only a few have focused on the gas properties of the lake ice cover. Here we present, to our knowledge, the first high resolution profiles of the total gas content and gas composition of lake ice from 4 lakes in Northern Sweden. This approach enables us to discuss gas enclosure in lake ice during the ~~whole~~3 months period of ice growth prior to ice cores collection. In this pilot study, ~~i~~Interactions between the water column and the ice cover as well as the intra- and inter-lake variability in hydrodynamic regimes are also shown to control bubbles composition, although a larger number of study cases is clearly required to quantitatively assess these relationships. ~~as well as the intra-and inter-lake variability in hydrodynamic regimes.~~

2 Study area and sampling

The four investigated lakes are embedded in the Stordalen Mire peat bog area (68°21' N, 19°02' E), near the Torneträsk lake (Figure 1). It is a sporadic or discontinuous permafrost area (Akerman and Johansson, 2008; Johansson et al., 2006a, 2006b) with low vegetation (Sonesson et al., 1980; Svensson et al., 1999). Transects from the center to the bank have been performed for each lake, in order to study the intra-lake variability. Ice cores were extracted along these transects. Several of these were analyzed for their gas properties. In this paper, we present 3 cores from Lake 2, and 4 cores from the other lakes. Figure 2 shows the ice cores locations, ice thickness and the depth profiles at times of core retrieval. We also collected about fifteen individual “ice embedded large flat bubbles”. These were ranging from 2 to 5 cm in diameter and were outcropping near the surface, but not especially along the studied transects~~studied~~. While Lake 1 and Lake 4 appear disconnected from any obvious water circulation pattern, Lake 2 and Lake 3 are not. We will refer to this contrast by using the “closed” vs. “open” lake terminology, respectively. Lake 1, Lake 2 and Lake 3 display a small surface area of 0.01 to 0.02 km². Lake 4 is quite larger (0.19 km²). According to water connections in the winter, Lake 1 is closed. Lake 2 has a semi-open character because of its

connection to another lake downstream (see Figure 1). Its profile hasn't been documented here-in details here, but its maximum depth is known to be 5 meters (Kokfelt et al., 2009). Lake 3 is relatively deep (5m) for its size. It is an open system as it benefits from water fluxes throughout the winter. Incoming water originates from the river (see Figure 1), and flows into the NW-lake to the West (pers. com. David Olefelt). Lake 4 consists of three interconnected areas and seems to behave as a closed system. Only the southern area has been studied in this paper. There, the lake is shallow with a maximum surveyed-depth of 105 cm.

The lake ice was drilled at the end of the winter in the last days of March 2008, near to maximum ice extent-and thickness.

3 Methods

The drilling was performed using a SIPRE-type ice auger (7.5 cm in diameter), the samples were cut with a band saw in a -20°C cold room. Horizontal thick sections (± 8 cm x 7 cm x 0.5 cm) were processed continuously along the ice cores using a Leitz 1400 microtome following the standard procedures from Langway (1958).

Gases entrapped in the ice were analysed every 5 cm (30g – 50g) for their total volume and composition (CO₂, O₂, N₂ and CH₄). Gas composition was measured by gas chromatography (Interscience Trace GC) using a FID detector for CO₂ and CH₄ and a TCD detector for O₂ and N₂. The gases were collected using the dry-extraction technique (extraction by crushing under vacuum (10^{-3} Torrs) and at low (-50°C) temperature) described in Raynaud et al. (1982) and Barnola et al. (1983). Precision of the measurements is 2.5% for CO₂, 0.4% for O₂ and N₂, and 3% for CH₄.

Total gas content was determined using a Toepler pump, applying the melting-refreezing extraction technique described in Martinerie et al. (1994). This system consists in placing a cubic ice sample with length of about 4 cm into an hermetic vessel thoroughly evacuated (10^{-3} Torrs). The Toepler pump extracts, collects and measures the volume of all gases present in the vessel after the ice had been melted (hot water bath) and slowly refrozen from the bottom, in order to reject all gases during the new ice formation. The associated total gas volume error is $\leq 5\%$ for ice containing small spherical bubbles as in glacier ice. This error can be largely increased for cylindrical bubbles (as observed in lake ice) since part of them can be open by cross-cutting during the sample preparation. The amount of gas lost can be estimated using calculation developed in Martinerie et al. (1990) and is depending of the

length, width and spacing of the cylindrical bubbles. In our case, the proportion of loss from the cylindrical bubbles varies between 20% and 90% for bubbles lengths of 0.6 cm and 3.2 cm respectively.

Ice thickness and depth measurements were performed with an ice thickness gauge designed (precision: ± 1 cm) by © Kovacs, an American company specialized in ice drilling and coring equipment.

4 Results

4.1 Ice characteristics

Figure 3 summarizes the ice and bubbles morphology from the 15 studied ice cores, as seen in transmitted light through the 0.5 cm thick sections. Visually, bubble shapes show a large variability. However, 6 major ice types have been identified, ~~on the basis of their~~ from bubble characteristics. Type 1 is peculiar and scarce, we call it “snow ice”, because this ice type ~~clearly~~ results from liquid water infiltration and refreezing in the snow cover at the lake surface. We observed this ice type at the very top ~~of few millimeters of most cores, but especially~~ core 1 on Lake 3. Type 2 corresponds to ice without visible bubbles. We will refer to it as “clear ice”, and it has been found in most part of the Lake 3 ice cover but also in small sections of Lake 1 and Lake 2 cores. Ice with elongated cylindrical bubbles (ice type 3) is predominant in Lake 4 (e.g. around 40 cm depth) but also in some sections of Lake 1 and Lake 2. Ice with spherical or nut shape bubbles is found at the bottom of all the shallow depths cores of Lake 1. Note that this ice type 4 is quite rich in bubbles.

Some core sections clearly display a mixture of cylindrical, spherical, and nut shaped bubbles as for example, section 47-65 cm depth in core 6 of Lake 1. This fifth ice type is called “mixed ice”. Finally, as described earlier in the paper, we can sometimes observe a sixth ice type ~~which contain~~~~se~~~~ontaining~~ bigger isolated large flat bubbles (see, top of core 2 in Lake 1). These bubbles can be very large with a diameter of up to a meter and are generally filled up by small hexagonal ice crystals, giving a whitish appearance to the bubble. These crystals, resulting probably from the inverse sublimation process after bubbles formation, reduce the gas volume in the latter. In this work, the maximum bubble size analyzed was obviously constrained by the corer diameter.

The genesis of the various ice types described above will be discussed further in this paper, but we would like to emphasize at this stage how the spatial distribution of these ice types varies within each lake as well as in between them. In Lake 1, the bubble content drastically increases between 50 cm depth and the bottom of cores 2, 4 and 6 where we find ice type 4 and 5. This feature does not exist in core 9, sampled above deeper water (Figure 2), where the bottom part is made of “clear ice” (ice type 2). Of all lakes studied, Lake 3 shows the lowest bubble density. It predominantly consists of ice type 2 (clear ice) except for two discrete zones with cylindrical elongated bubbles (around 30 cm depth and at the top of core 8) (Figure 3). The sub horizontal lines in core 1 from the same lake are not bubble but natural fractures. Lake 4, which is nearly frozen to bottom along the whole profile (Figure 2), on the contrary, shows a large density of bubbles for all cores at all depths, dominated by ice type 3 (elongated bubbles) and mixed ice (ice type 5). Finally, in all of the 15 ice cores for which thick sections have been made, we can identify a common zone of higher bubble density at about 30 cm depth (Figure 3).

4.2 Gas composition

~~Gas composition has been measured continuously and~~ Spatially continuous gas composition measurements have been performed at high resolution (5cm) in a selected core ~~for of~~ each lake (cores 4, 1, 1 and 4 for respectively lakes 1, 2, 3 and 4); ~~We but also measured the gas composition within the in individual samples of the~~ large flat bubbles of (ice type 6). Results are presented in ~~F~~figure 4.

Methane mixing ratios (Figure 4a) vary largely between 3 ppm and 47%. Large flat bubbles show the maximum mixing ratios whereas profiles values are at the level of tens to hundreds of ppm with a few peaks around 10 ~~or to~~ 20%. We observe an increase for all lakes (except for Lake 3) around 25 cm depth. Methane mixing ratios for lakes 1 and 4 increase with depth whereas the mixing ratios of lakes 2 and 3 remain low.

Unlike methane, the range of CO₂ mixing ratios (Figure 4b) is the same for the large flat bubbles (ice type 6) as for the ~~cores~~ profiles (between 200 and 4000 ppm)~~in the cores. To~~ ~~One the single exception is snow ice at the very of the top of the lake 3 core 1 (9%), it varies between 200 and 4000 ppm.~~ For all lakes, however, the CO₂ mixing ratio increases with depth with a maximum value of 46 600 ppm.

Oxygen mixing ratio (Figure 4c left) is about 20% near the surface of all lakes, to the exception of some large flat bubbles with lower values at 10 %. In Lake 1, 2 and 4, there is

also a relative minimum at 10-15% around 25 cm depth and a clear decrease again between 40 cm depth and the bottom of the cores to mixing ratios of 5 to 15%. Lake 3, on the contrary, is remarkably stable at a value of 21%, close to the atmospheric value, although with very low total gas content (see Figure 4e and section 4.3.).

Nitrogen mixing ratios (Figure 4c right) are around 78% near the lakes surface and, in most cases, logically evolve as mirror-image of ~~in opposition to~~ the O₂ mixing ratio (since ~~they- these two species~~ are usually the dominant species in the mix).

The O₂/N₂ ratio (Figure 4d) varies between 0.084 and 0.33 for ice type 6 and between 0.26 and 0.34 for the cores profiles near the lakes surface. The ratio decreases with depth to a minimum value of 0.05 for Lakes 1, 2 and 4 whereas it remains constant for Lake 3 with a value of 0.28. The decrease of the ratio actually always reflects a decrease in the oxygen, which is confirmed by a comparison of O₂ and N₂ concentrations in the water (not shown). For Lake 1, 2 and 4 repeated changes of the ratio are seen throughout the depth, superimposed to the general trend.

4.3 Total gas content

The total gas content results of Figure 4e should ~~be taken with care and~~ generally be considered as ~~a~~-minimum values. As discussed in the method section, ~~The~~-the extraction process indeed underestimates the total gas content from the samples, by cutting through bubbles on sampling and therefore losing part of their gas content. This error becomes significant for ice with cylindrical elongated bubbles (between 20% and 90% for bubbles length about 0.6 cm and 3.2 cm respectively) and it is difficult to determine the ratio of each bubble length for a given sample. ~~On the other hand, we do not show values for ice type 6 since it clearly has no meaning (single isolated bubbles).~~

This being said, our values are in the same range or slightly higher than other studies previously performed on lake ice (e.g. Lorrain et al., 1999, 2002). Note also that values above the maximum equilibrium dissolved gas content of fresh water (about 0.023 ml g⁻¹_{ice}) are also observed in lakes 1 and 2.

We do not show values for ice type 6 since this has no meaning (single isolated bubbles).

5 Discussion

5.1 A new lake ice type classification based on bubbles properties

Bubble formation processes and shapes in lake ice have already been discussed at length by several authors (Adams et al., 1998; Bari and Hallett, 1974; Carte, 1961; Gow and Langston, 1977). These authors suggest that bubble shapes and density will result from a balance between the ice growth rate of advance of the freezing front, and the diffusion of rejected solubility state of the gases in the liquid reservoir ahead. Basically, as the ice grows, most of the gases remain dissolved in the water since gas solubility in ice is at least 2 order of magnitude smaller than in water (Killawee et al., 1998). With a faster freezing front, bubbles will form and be rather elongated and perpendicular to the ice front. They can sometimes be accompanied by “nut shape” bubbles. At low freezing rates, the ice can be devoid of bubbles if the expelled gases are able to diffuse and dissolve in the water reservoir. Furthermore, finally another type of bubbles is commonly encountered in lake ice covers of permafrost areas. It originates from sediment degassing, large bubbles resulting from sediment degassing will also be a common feature (Walter et al., 2006) and consists of large flat bubbles trapped within the ice as it grows around.

The data collected in this paper enable us to propose a new “process-driven” lake ice type classification based on bubbles characteristics and associated gas composition. This classification, summarized in Figure 5, combines the influence of dissolved gases in the water, sediment degassing and gas-water interactions within the water column. It differs from the one established by Walter et al. (2006), mostly by in that the bubble size ranges that we address are different. Indeed, in this work, we are limited by the sampling method to bubbles that are smaller than 5 cm in diameter. Each of the 6 ice types described in section 4 and Figure 5 can then be associated to a specific genetic process for the bubble inclusions. Type 1 (snow ice) is formed by liquid water infiltration in blown snow blown at the surface of the lake and subsequent refreezing. Type 2 (clear ice) is typical of lake ice formed in conditions of slower freezing (favouring diffusion ahead of the freezing front) of a water reservoir which is undersaturated or not supersaturated enough for bubble nucleation to take place. Type 3 (elongated bubbles) and 4 (spherical and nuts shape bubbles) is typical lake ice where bubbles solely result from the capture of exsolved gases as the boundary layer ahead of the ice-water interface gets strongly supersaturated from impurity rejection by the ice (higher freezing rates, closed system freezing). Type 6 ice (large flat bubbles) is the signature of an

ebullition process from the sediment on the lake floor, captured at the base of the ice cover. Finally, type 5 is the expected mixed facies when both exsolution and ebullition contribute to the bubble content at the same location.

5.2 Depth dependency of the gas composition

In parallel with the different bubble characteristics of the various ice types, the composition of these gaseous inclusions varies with depth in most cases. Figure 4c, for example, shows a clear decrease of the oxygen mixing ratio from 20% near the surface to about 5 to 10% at 70 cm depth. Simultaneously, the CO₂ mixing ratio increases from 500-1500 ppm up to a maximum value of 40 000 ppm. Oxygen ~~depletion with depth decrease~~ is a known phenomenon in stratified lakes (e.g. Casper et al., 2000) and generally attributed to respiration processes ~~in the liquid phase~~.

In order to decipher the impact of ~~biogenic-biogeochemical~~ processes from the mere ~~physical~~ evolution of gas properties under the specific hydrodynamic conditions of a freezing lake, we have estimated the evolution of gas concentration in water (mol l^{-1}) and of gas mixing ratios (ppm, %) in water and ice, ~~in the absence of biological activity~~, using the simple following approach. ~~We hypothesize~~ ~~Hypothesizing~~ that the initial gas composition of the lake water is in equilibrium with the atmosphere for O₂, N₂ and CH₄ and showing a pCO₂ of 600 ppm as measured by Jonsson et al. (2007) in early autumn for lakes in our study area. We ~~further assume, and~~ that the reservoir evolves as a closed system ~~and that no supersaturation persist for a significant period of time before bubbles nucleation takes place, one can~~ We then compute, using Henry's law (eq. 1) and the total gas content measured in the ice (Figure 4e), the theoretical evolution of gas concentrations (mol l^{-1}) in the ~~water~~ reservoir with depth ~~at all times~~ applying a simple mass balance between ice and water (Figure 6). This is shown as white diamonds for oxygen, carbon dioxide and methane in Figure ~~6-7~~ (nitrogen not shown).

$$c = k_h \cdot p \quad (1)$$

Where c = dissolved gas concentration (mol l^{-1})

k_h = Henry's constant ($\text{mol l}^{-1} \text{ atm}^{-1}$)

p = gas partial pressure (atm)

k_h values and temperature corrections were applied as recommended in Sander's review (1999). Further, theoretical mixing ratios in water and ice (using Henry's law again) can be reconstructed (Figure 6), as shown for all gases in Figure 78.

1 A specific approach has been adopted in the case of carbon dioxide to take into
2 account the evolution of the carbonate system as freezing occurs. Observed autumnal ranges
3 (Jonsson et al. 2007) of $p\text{CO}_2$ (around 600 ppm) and of total dissolved inorganic carbon (DIC
4 - around $100 \mu\text{moles kg}^{-1}$) have been used in the USGS version of the CO2Calc program
5 (Robbins et al. 2010) to assess the initial alkalinity (TA) of the water reservoir before
6 freezing. CO2Calc was then used iteratively to recalculate equilibrium $p\text{CO}_2$ (and therefore
7 mixing ratio in the newly formed bubbles) from updated TA and DIC at each freezing step,
8 taking into account the amount of DIC stored as CO_2 bubbles in the newly formed ice. Used
9 settings for the CO2Calc program were: salinity = 0‰, temperature = 0°C , Pressure = 1 atm,
10 K_1 and K_2 from Millero 1979, $\text{KHSO}_4 = \text{Dickson}$, pH scale = NBS scale.

11 This theoretical model is clearly a simple theoretical reference scenario treating gases
12 as passive tracers in that: a) no water mass advection from other lakes is allowed, b) bubbles
13 nucleation is occurring as soon as maximum solubility is reached, c) selective diffusion ahead
14 of the freezing front is neglected (which might affect the mixing ratios by a maximum factor
15 of 2 to 3 in the early stages of freezing (high freezing rates, top layers) and d) surmised
16 homogeneization of the gas rejected in the reservoir will be potentially partly hampered due to
17 the temperature-driven density stability of the water column (increasing the potential
18 supersaturation at the ice-water interface). Note however that the latter should not affect our
19 results since we use the observed total gas contents in the ice (as opposed to a parametrization
20 of ex-soluted gases from the level of supersaturation) and since the potential absence of
21 physical mixing should affect all gases in the same way (therefore not altering the mixing
22 ratios deduced from gas concentrations in the new water volume - Figure 6). ~~Note that these~~
23 ~~computations neglect potential selective diffusion ahead of the freezing front, which might~~
24 ~~affect the results by a factor of 2 to 3 at high freezing rates (top layers), considering respective~~
25 ~~diffusion coefficient of various species. Care should also be taken in discussing these curves~~
26 ~~in the specific case of carbon dioxide, since our calculations did not take into account the re-~~
27 ~~equilibration of the carbonate system in the water, as freezing concentrates carbon dioxide in~~
28 ~~the remaining reservoir. Indeed, at normal pH, the major part of carbon dissolved in the water~~
29 ~~is under the HCO_3^- form. Our theoretical CO_2 curves in Figures 6 and 7 based on a simple~~
30 ~~conservative mass balance between ice and water in a closed system therefore potentially~~
31 ~~overestimate the increases of CO_2 concentrations in water and the mixing ratios in water and~~
32 ~~ice as the reservoir closes.~~

Despite these limitations, our theoretical curves of Figure 76 and 87 allow us to put forward potential discrepancies due to either open system conditions or biogeochemical processes.

As expected from the limited amount of gas enclosed as bubbles in the ice, theoretical concentrations in water regularly increase with depth (Figure 76, N₂ not shown). Also, following relative solubilities, mixing ratio increase for all gases ~~apart from~~ but nitrogen, as as ~~nitrogen is since the latter is~~ the dominant species and the least soluble species (Figure 87a). Maximum theoretical water concentrations are reached at the bottom of Lake 1 with value of ~~5.25.0~~ ppm in CH₄, ~~55-00086 000~~ ppm in CO₂ and ~~5554~~% for O₂, resulting in ice bubbles mixing ratios of ~~respectively~~ 3.2 ppm, ~~1100-2600~~ ppm and 36.9%, respectively. Another salient feature of Figure 87 is the behavior of Lake 3 showing only little changes with depth, as expected from its deeper waters (Figure 2).

~~Now, real~~ Real gas concentrations in the water can also be reconstructed using the ~~observed-measured~~ gas mixing ratios in the ice and applying Henry's law. This is shown for O₂, CO₂ and CH₄ as grey triangles ~~downwards~~ in Figure 76.

Are the observed ice gas mixing ratio profiles of Figure 4 then coherent with the closed system theoretical evolution shown in Figure 87b? Methane shows a wide range of values (from a few ppm to 100 000) and no systematic increasing trend with depth. Only exceptionally is the maximum "closed system" value of a few ppm observed (here as a minimum in the profiles), and not necessary at the bottom of the ice cover. This clearly suggests that exsolution is not the dominant process in controlling methane mixing ratios in the ice, but rather the varying contribution of ebullition process.

Comparing observed to theoretical profiles for carbon dioxide in lakes 1, 2 and 4 shows a similar trend of increasing mixing ratio in ice (Figure 87b) and concentrations in water (Figure 76, middle panel). However, again, in both cases, observed values can be higher than theoretical ones by up to an order of magnitude, with considerable superimposed variability. An additional source of carbon dioxide is therefore required, and this from the very beginning of the growth season as shown by the lake water supersaturation level of the reconstructed water concentrations from bubbles in the ice (Figure 67, central panel, ~~grey diamonds~~). Could this be the result of respiration processes in the reservoir? The behavior of dissolved oxygen is worth considering in that respect. Indeed, instead of showing the expected increase of mixing ratio (Figure 87a) and concentration in water (Figure 76, left panel, white diamonds) with depth, reconstructed water concentrations actually slightly decrease in lakes

1, 2 and 4. This could be interpreted as the signature of respiration. Looking at relative increase of CO₂ and decrease of O₂ in Figure 76 reveals important contrasts between lakes and between depths in a given lake. In the lower half of lakes 2 and 4 oxygen loss and CO₂ gain are in relative balance, which does not preclude a respiration control in the water column during ice growth, ~~especially that we know that some of the CO₂ produced could have moved to the HCO₃⁻ pool.~~ On the contrary, in the upper half of the ice cover from the same lakes, negligible amounts of oxygen are lost, whilst excess carbon dioxide is present. For Lake 1, CO₂ gain is at all times in excess of the O₂ loss, also suggesting an alternative source to respiration for CO₂, from the very beginning of the lake ice growth. Finally, Lake 3, which has been described as a relatively open system, shows three distinct sections; a lower one coherent with ~~episodic~~ respiration processes ~~(as in lakes 2 and 4)~~ and returns to a fully open system regime, a top section where the CO₂ gain overwhelms the (negligible) O₂ loss (as in all other lakes), and a middle section where CO₂ concentrations are ~~closed to the theoretical closed system evolution~~ again what would be expected from open system conditions.

To summarize, dissolved CO₂ concentrations in the waters of lakes 2, 3 and 4 ~~can~~ could be explained by “in situ” respiration processes for waters generating the lower part of the lake ice cover (late growth), whilst an extra source (as compared to simple equilibrium with atmosphere) is needed for the waters generating the upper part of the lake ice cover (early growth). For Lake 1, this extra source is needed at all times. Although reservoir closure is unable to explain the observed levels of ~~water~~ concentration, it could be partly responsible for the general trend of CO₂ concentrations in lakes 1, 2 and 4.

Several mechanisms, other than respiration, ~~can~~ could be responsible for ~~explain~~ the high levels of observed dissolved CO₂ in our lake waters. Gas ebullition from the sediment can certainly contribute to the CO₂ increase. Sulfato-reduction, which is often associated to the methanogenesis process (Fenchel et al., 1998), is also a provider of carbon dioxide. ~~and~~ The particular smell of H₂S, another by product of the reaction, has been detected ~~in the course of sampling during the field trip.~~ Denitrification, methane oxidation or acetate fermentation can also contribute to the CO₂ content (Stumm and Morgan, 1996). In our case, the similarity of the reconstructed CH₄ and CO₂ concentration profiles in water in most lakes (Figure 76, middle and right panels) suggest that acetate fermentation might be the dominant extra CO₂ source at work, as opposed to methane oxidation. This also puts forward acetate fermentation as the source for methane. δ¹³C and δD isotopic analysis of the CH₄ would of course help in deciphering the sources, but these unfortunately and not available at this time.

1 The generalized CO₂ excess in the surface layer of all lakes could reflect the dynamical
2 instability of the lake waters in the autumn, bringing bottom enriched waters to the lake
3 surface just before the onset of freezing.

4 The O₂/N₂ ratio (Figure 4d) ~~actually~~ reflects the changes in the oxygen mixing ratio
5 and can therefore ~~also~~ be used as an indicator of the stratification process in the lake during
6 the winter. ~~However~~ But, it can also be a measure of the hydrological regime in the lake (open
7 vs. closed system). For example, Lake 3 shows a constant O₂/N₂ ratio throughout the depth
8 because the input of atmosphere equilibrated waters from the river upstream (Figure 1)
9 inhibits the changes in oxygen mixing ratios due to the ice cover freeze on (closure) or
10 biological processes as discussed above. It is interesting to note that local CO₂ mixing ratio
11 increases occur at about 50 and 60 cm depth, despite the water circulation. This suggests that
12 these excursions correspond to local ebullition events, as confirmed in the CH₄ profile.

13 5.3 Ice type dependency of gas mixing ratios

14 Figure 5 shows contrasted CH₄ and CO₂ signatures for the various ice types described in
15 section 5.1. Only one measurement is available for the “snow ice” (type 1), and it shows the
16 highest CO₂ value of the whole study at 90 000 ppm. This is hard to explain by physical
17 processes only. Figure 87a shows that CO₂ values up to ~~54 000~~ 86 000 ppm can be reached for
18 gas dissolved in water during closed system freezing of lake reservoir (at about 70%
19 freezing). Bulk freezing of residual water from the final stages of closed system freezing of a
20 lake, expelled at the surface through the moat and bathing the snow cover, could therefore
21 lead to such high CO₂ values. This is however quite unlikely, since our “snow ice” was
22 measured at the surface of Lake 3, which was the least “closed”. Bacterial respiration of
23 organic matter blown with the snow at the lake ice surface is another plausible explanation.
24 Strangely enough, oxygen does not show the expected concentration decrease if aerobic
25 respiration had been active. Ice types 2 to 4 should span the range of theoretical CO₂ mixing
26 ratios shown in Figure 87b (~~400-600~~ to ~~1100-2600~~ ppm) if the water was initially ~~with a pCO₂~~
27 ~~about 600 ppm in equilibrium with the atmosphere~~. We know from the discussion above that
28 this is not true, and the observed range of 3000 to 4000 ppm is in accordance with ex-solution
29 from a lake water displaying the observed excess-CO₂ concentration. The “mixed ice” (type
30 5), with apparent contribution from both exsolution bubbles and small bubbles resulting from
31 sediment ebullition, shows higher CO₂ and CH₄ mixing ratios as compared to ice type 3 and
32 4. This suggests that the small bubbles coming from the sediment contribute to increase both

the carbon dioxide and the methane content as surmised from the discussion in the previous section. The large flat bubbles (type 6), also derived from sediment ebullition are globally richer in methane but poorer in carbon dioxide. This however does not mean that the amount of carbon dioxide in these bubbles is lower as compared to ice type 5, since the data are shown as mixing ratio (i.e. relative concentration). It is nevertheless disturbing, if ice type 5 is a mixture between ice types 3/4 and 6, that the CO₂ mixing ratio is not at an intermediate value (as does CH₄ in Figure 5). This suggests that a small fraction of methane (not detectable in Figure 76) might have been oxidized to CO₂ in the lake environment ~~or in the ice itself~~. Finally, it is striking that, although they show an increasing mean/median methane concentration value, ice types 4, 5 and 6 display similar (large) concentration ranges. This probably reflects the combination of increased supersaturation of the ex-soluted waters in the nearly closing reservoir (ice type 4) and direct ebullition from the sediment nearby (ice type 6).

Our results globally underlines that the lake ice cover signature is ~~clearly different~~ far from ~~from that of being governed by pure ebullition only~~. As illustrated by the contrast between ice type 5 and 6, the least soluble methane dominates ebullition, while carbon dioxide mixing ratio is higher in the lake ice storage. Clearly, our data indicate that exsolution dominates the lake ice cover signature. Further, the fact that methane mixing ratios observed in bubble type 6, the closest to pure ebullition, are still largely lower than those observed in studies of pure ebullition fluxes, indicates that substantial exchanges with dissolved gases occurred for those ice entrapped ebullition products. This however needs to be weighed, in terms of budget, by the overwhelming amount of gas liberated through ebullition, as compared to the one stored in the lake ice.

5.4 Controls on bubble distribution in lake ice

Intra-lake and inter-lake comparison in our dataset shows that there is a control of geometry on the bubble distribution in the ice, which is of potential interest in the perspective of upscaling regional dataset to global carbon budgets. For ~~example instance~~, the proximity of the bottom of the lake increases the amount of bubbles in the ice. Figure 2 and 3 indeed show that the lower part of cores C2, C4 and C6 of Lake 1 (in shallow areas) is rich in bubbles while ~~it is not true for~~ core C9, (located above deeper waters) is not. ~~For~~ Lake 4 ~~which~~ is shallow and nearly frozen to the bottom ~~and its all~~ ice cores are bubble rich. This suggests that shallow lakes will enclose more gas in the ice cover. ~~not only the surface area of the lakes (Bastviken~~

~~et al., 2004; Juutinen et al., 2009), but also their water depth is important in assessing gas productivity on a larger scale. Other factors such as the amount of organic matter locally available or the sedimentation rate would of course further affect the gas fluxes from the sediment, but these were not documented in the present data set.~~

The hydrological regime of the lake system can also directly impact the gas content in the lake ice. Our study shows that if a lake is part of an open drainage system, the ice can be nearly devoid of gas. Lake 3, which is fed by a river (Figure 1), and where the water drains into another lake, is a good example (Figure 3). The three other lakes, on the contrary, are closed or open to another lake without significant water circulation and all show a significative bubble content. In the first case it would be adequate to investigate if the lack of bubbles in the ice is counterbalanced by a supplementary provision in the connected lakes, and to understand how they will affect the quantity (fluxes) and the quality (CH₄ vs. CO₂) of the gases released to the atmosphere.

~~Finally, in this study,~~The proximity of the lake banks “~~bank proximity~~” does not seem, ~~in our data set,~~ to affect the bubble distribution despite the fact that lakes can be more methane productive along lakes margins (e.g. Walter et al., 2007). However, all lakes are relatively small, and the situation might be different for larger lakes.

Local events of atmospheric pressure dropping has also been claimed to trigger bubble ~~nucleation-production~~ in lake ice (Mattson and Likens, 1990; Semiletov, 1999). In this study, we observed two simultaneous bubbling events for the 4 lakes, the first one around 30 cm depth (well documented in Figure 3) and the second around 60 cm (clearly seen during cores handling). To investigate a potential relationship of these events to marked atmospheric pressure changes, we first need to reconstruct a time line for the buildup of the lake ice cover. A simple (neglecting geothermal heat flux) thermodynamic model for freezing (Hinkel, 1983) has been run, based on equation 2:

$$\rho_i \lambda \frac{\partial Z_i}{\partial t} = \frac{(T_0 - T_s)}{\left(\frac{Z_i}{K_i} + \frac{Z_s}{K_s}\right)} \quad (2)$$

Where ρ_i = density of ice (kg m^{-3})

λ = latent heat of fusion (J kg^{-1})

Z_i = ice thickness (m)

Z_s = snow thickness (m)

1 $K_i = \text{thermal conductivity of ice } (W m^{-1} ^\circ C^{-1})$

2 $K_s = \text{thermal conductivity of snow } (W m^{-1} ^\circ C^{-1})$

3 $T_0 = \text{temperature at ice/water interface } (^\circ C)$

4 $T_s = \text{surface temperature } (^\circ C)$

5 $t = \text{duration of constant } T_s \text{ (s)}$

6 The model reconstructs the ice thickness Z_i as a function of ~~the temperature changes and this~~
7 from the first day of freezing. It has been run both with and without a snow cover to obtain a
8 reasonable prediction of the evolution of the ice cover. The snow cover ~~data set deduced from~~
9 ~~snow fall events, from the nearby weather station doesn't account for snow redistribution at~~
10 ~~the surface of the lakes. Therefore the model has been run both with and without a snow cover~~
11 ~~to obtain a reasonable prediction of the evolution of the ice cover. was however quite variable~~
12 ~~between lakes depending on exposition, wind and sublimation processes. It is From those~~
13 ~~runs, we have possible to~~ correlated in Figure 9 (hatched area) the observed major bubbling
14 events at around 30 and 60 cm depth with major occurrences of atmospheric pressure drops
15 ~~on Figure 8 (hatched areas)~~. This confirms that attention should be drawn to major
16 atmospheric pressure events in assessing methane release efficiency from ~~periglacial-boreal~~
17 lakes.

18 **5.5 Assessing a lower bound for lake ice melting contribution to the** 19 **atmospheric methane budget**

20 In this section we present a “back of the envelope” calculation for a minimum winter
21 contribution of periglacial lakes to methane fluxes to the atmosphere. We rely on our ice
22 type/bubbles classification to perform a budget for methane accumulation in lake ice during
23 the winter. We first calculate the proportion of each ice type in each core considering it as
24 representative for the whole lake ice cover. We then multiply this proportion by the minimum,
25 mean (median) and maximum CH_4 mixing ratio for this type of ice and by the observed mean
26 total gas content of the given ice type. This provides an ice-type weighed concentration of
27 methane in ml CH_4 per gram of ice for each lake. This value is then integrated over the lake
28 ice mass and divided by the lake area and by the number of days ~~of existence of~~ the ice cover
29 ~~existed~~. Results are presented in Table 1. Although these values do not represent the actual
30 flux of methane to the atmosphere during the relatively short melting period, they provide a

mean winter daily flux, that can be more easily compared to spring-summer flux estimates available in the literature.

We consider these values as minimal for two reasons: a) because the total gas volume measurements were probably biased towards gas losses (see subsection 4.3), and b) because we cannot include the contribution of bubbles above 5 to 6 cm in diameter, which are most likely the larger contributors to the methane budget (Walter et al., 2010). We however consider our results as a measure of the “background contribution” of permafrost lake ice; without the big bubbles events. This work is therefore complementary to other studies focusing on large methane emission observed in spring, due to the ice cover melting and water turnover which releases the excess dissolved gases stored in the water column (Michmerhuizen et al., 1996; Phelps et al., 1998). It is also complementary to studies focusing on larger bubbles in winter lake ice (e.g. Walter et al., 2006, 2007, 2008, 2010).

Our results present a large variability between each lake. Lake 1 shows values ($1.34 \cdot 10^{-3} - 12.7 \text{ mg CH}_4 \text{ m}^{-2} \text{ d}^{-1}$) comparable ~~with some~~ other studies (Bastviken et al., 2004; Kling et al., 1992; Repo et al., 2007; Rudd et al., 1993; Zimov et al., 2001) reporting values from 0.3 to 77 $\text{mg CH}_4 \text{ m}^{-2} \text{ d}^{-1}$. Lakes 2, 3 and 4, on the contrary, show values from $6.52 \cdot 10^{-5}$ to $4.4 \text{ mg CH}_4 \text{ m}^{-2} \text{ d}^{-1}$ which are in the lowest range of those reported in most studies on methane fluxes from lakes (values observed from 0 to $3240 \text{ mg CH}_4 \text{ m}^{-2} \text{ d}^{-1}$; Walter et al., 2010). We did expect to find moderate contribution from lake ice in the winter, but we show here that these are not negligible and worth considering in global budget estimations.

6 Conclusions

This work contributes to the study of methane released from lakes in periglacial environments. It provides new results on the winter gas storage associated to the lake ice cover buildup. A new genetic lake ice types classification is proposed, based on bubbles shapes, density and gas composition. It is used to provide a first minimal estimate of methane fluxes associated to winter storage in the lake ice cover, which are complementary to previous studies focusing on spring and summer fluxes from open water sources and studies focusing on large bubbles in lake ice. It is shown that although moderate, as expected, these fluxes are not negligible with respect to other sources.

Gas composition study of the bubbles reveals strong supersaturation of the lake water both in methane and carbon dioxide, especially in the lakes that evolve in near closed system.

1 These high concentrations are thought to mainly result from interaction with biological
2 processes in the sediment, of which acetate fermentation would be a likely candidate, given
3 the observed synergy between CO₂ and CH₄ in the profiles. Part of the excess CO₂ could also
4 result from respiration processes, as indicated by oxygen losses, especially during the second
5 half of the ice growth period. Mere closure of the lake reservoir cannot explain the observed
6 concentration excess, but could be partly responsible for the global trend of increasing
7 concentrations with depth in the water and in the ice.

8 We also demonstrated that lakes geometry and hydrological regime affect the amount
9 and characteristics of gases enclosed in the ice, **although this pilot study obviously does not**
10 **have yet the statistical power to derive quantitative relationships**. Finally, we confirm that
11 atmospheric pressure regimes can trigger bubble nucleation and sediment ebullition events
12 and therefore should ~~indeed~~ be considered as a factor in methane release efficiency.

13 Future work will focus on the stable isotope composition of the bubbles in the
14 different ice types, in order to decipher the relative importance of physico-chemical and
15 biologically mediated processes in controlling the gas properties in permafrost lake ice.

17 **Acknowledgements**

18 We thank the Abisko Scientific Research Station (ANS) in Sweden for their grant and the
19 weather data, the "Fonds de Service pour la Recherche Glaciologique Polaire de l'Université
20 Libre de Bruxelles" and the "Crédits pour Brefs Séjours à l'étranger" of the FNRS for the
21 financial support. We thank Kristina Bäckstrand and David Olefelt for their field knowledge
22 and the personal communications.

24 **References**

25 Adams, E. E., Priscu, J. C., Fritsen, C. H., Smith, S. R. and Brackman, S. T.: Permanent ice
26 covers of the McMurdo Dry Valleys lakes, Antarctica: bubble formation and metamorphism,
27 in Ecosystem Dynamics in a polar desert: the McMurdo Dry Valleys, Antarctica, edited by J.
28 Priscu, pp. 281-295, American Geophysical Union, Washington, DC., 1998.

29 Akerman, H. J. and Johansson, M.: Thawing Permafrost and Thicker Active Layers in Sub-
30 arctic Sweden, Permafrost and Periglacial Processes, 19, 279-292, 2008.

1 Bari, S. A. and Hallett, J.: Nucleation and growth of bubbles at an ice-water interface, *Journal*
2 *of Glaciology*, 13(69), 489-520, 1974.

3 Barnola, J. M., Raynaud, D., Neftel, A. and Oeschger, H.: Comparison of CO₂ measurements
4 by two laboratories on air from bubbles in polar ice, *Nature*, 303, 410-413, 1983.

5 Bastviken, D., Cole, J., Pace, M. and Tranvik, L.: Methane emissions from lakes: Dependence
6 of lake characteristics, two regional assessments, and a global estimate, *Global Biogeochem.*
7 *Cycles*, 18(4), GB4009, 2004.

8 Carte, A. E.: Air bubbles in ice, *Proceedings of the Physical Society*, 77(3), 757-768,
9 doi:10.1088/0370-1328/77/3/327, 1961.

10 Casper, P., Maberly, S. C., Hall, G. H. and Finlay, B. J.: Fluxes of methane and carbon
11 dioxide from a small productive lake to the atmosphere, *Biogeochemistry*, 49(1), 1-19, 2000.

12 Fenchel, T., King, G. M. and Blackburn, T. H.: *Bacterial biogeochemistry: The*
13 *Ecophysiology of mineral cycling*, Academic Press., 1998.

14 Gow, A. J. and Langston, D.: Growth history of lake ice in relation to its stratigraphic,
15 crystalline and mechanical structure, *USA CRREL Report (Cold Regions Research and*
16 *Engineering Laboratory)*, 77(1), 24p, 1977.

17 Hinkel, K. M.: Ice-cover growth rates at nearshore locations in the Great Lakes, *NOAA Tech.*
18 *Memorandum ERL GLERL*, 35, 1983.

19 IPCC: Intergovernmental Panel on Climate Change (IPCC), *the physical science basis*,
20 Cambridge Univ. Press., 2007.

21 Johansson, M., Christensen, T. R., Åkerman, H. J. and Callaghan, T. V.: What determines the
22 current presence or absence of permafrost in the Torneträsk region, a sub-arctic landscape in
23 northern Sweden?, *Ambio*, 35(4), 190-197, 2006a.

24 Johansson, T., Malmaer, N., Crill, P. M., Friborg, T., Akerman, J. H., Mastepanov, M. and
25 Christensen, T. R.: Decadal vegetations changes in a northern peatland, greenhouse gas fluxes
26 and net radiative forcing, *Global Change Biology*, 12, 2352-2369, 2006b.

27 Jonsson, A., Åberg, J., and Jansson, M.: Variations in pCO₂ during summer in the surface
28 water of an unproductive lake in northern Sweden, *Tellus B*, 59, 797-803, 2007.

29 Juutinen, S., Rantakari, M., Kortelainen, P., Huttunen, J. T., Larmola, T., Alm, J. and Silvola,
30 J.: Methane dynamics in different boreal lake types, *Biogeosciences*, 6(2), 209-223, 2009.

- 1 Killawee, J. A., Fairchild, I. J., Tison, J.-L., Janssens, L., and Lorrain, R.: Segregation of
2 solutes and gases in experimental freezing of dilute solutions: Implications for natural glacial
3 systems, *Geochemica et Cosmochimica Acta*, 62, 3637-3655, 1998.
- 4 Kling, G., Kipphut, G. and Miller, M.: The flux of CO₂ and CH₄ from lakes and rivers in
5 arctic Alaska, *Hydrobiologia*, 240(1), 23-36, 1992.
- 6 Kokfelt, U., Rosén, P., Schoning, K., Christensen, T. R., Förster, J., Karlsson, J., Reuss, N.,
7 Rundgren, M., Callaghan, T. V., Jonasson, C. and Hammarlund, D.: Ecosystem responses to
8 increased precipitation and permafrost decay in subarctic Sweden inferred from peat and lake
9 sediments, *Global Change Biology*, 15(7), 1652-1663, doi:10.1111/j.1365-
10 2486.2009.01880.x, 2009.
- 11 Koven, C. D., Ringeval, B., Friedlingstein, P., Ciais, P., Cadule, P., Khvorostyanov, D.,
12 Krinner, G., and Tarnocai, C.: Permafrost carbon-climate feedbacks accelerate global
13 warming, *PNAS*, 108, 14769-14774, 2011.
- 14 Langway, C. C. J.: Ice fabrics and the Universal stage, 1958.
- 15 Lorrain, R. D., Fitzsimons, S. J., Vandergoes, M. J. and Stievenard, M.: Ice composition
16 evidence for the formation of basal ice from lake water beneath a cold-based Antarctic
17 glacier, *Ann. Glaciol.*, 28, 277-281, 1999.
- 18 Lorrain, R., Sleewaegen, S., Fitzsimons, S. and Stievenard, M.: Ice formation in an Antarctic
19 glacier-dammed lake and implications for glacier lake interactions, *Arct. Antarct. Alp. Res.*,
20 34(2), 150-158, 2002.
- 21 Martinerie, P., Lipenkov, V. Y., and Raynaud D.: Correction of air-content measurements in
22 polar ice for the effect of cut bubbles at the surface of the sample, *Journal of*
23 *Glaciology*, 36, 299-233, 1990.
- 24 Martinerie, P., Lipenkov, V. Y., Raynaud, D., Chappellaz, J., Barkov, N. I. and Lorius, C.: Air
25 content paleo record in the Vostok ice core (Antarctica): A mixed record of climatic and
26 glaciological parameters, *J. Geophys. Res.*, 99(D5), 10565-10576, 1994.
- 27 Mattson, M. D. and Likens, G. E.: Air pressure and methane fluxes, *Nature*, 347(6295), 718-
28 719, 1990.

- 1 Michmerhuizen, C. M., Striegl, R. G. and McDonald, M. E.: Potential Methane Emission
2 from North-Temperate Lakes Following Ice Melt, *Limnology and Oceanography*, 41(5), 985-
3 991, 1996.
- 4 Phelps, A. R., Peterson, K. M. and Jeffries, M. O.: Methane efflux from high-latitude lakes
5 during spring ice melt, *J. Geophys. Res.*, 103(D22), 29029-29036, 1998.
- 6 Raynaud, D., Delmas, D., Ascencio, J. M. and Legrand, M.: Gas extraction from polar ice
7 cores: a critical issue for studying the evolution of atmospheric CO₂ and ice-sheet surface
8 elevation, *Annals of Glaciology*, 3, 265-268, 1982.
- 9 Repo, M. E., Huttunen, J. T., Naumov, A. V., Chichulin, A. V., Lapshina, E. D., Bleuten, W.
10 and Martikainen, P. J.: Release of CO₂ and CH₄ from small wetland lakes in western Siberia,
11 *Tellus B*, 59(5), 788-796, doi:10.1111/j.1600-0889.2007.00301.x, 2007.
- 12 Robbins, L.L., Hansen, M.E., Kleypas, J.A., and Meylan, S.C.: CO₂calc—A user-friendly
13 seawater carbon calculator for Windows, Mac OS X, and iOS (iPhone), U.S. Geological
14 Survey Open-File Report 2010–1280, 17 p. 2010
- 15 Rudd, J. M. ., Harris, R. and Kelly, C. A.: Are hydroelectric reservoirs significant sources of
16 greenhouse gases?, *Ambio*, 22(4), 246-248, 1993.
- 17 Sander, R.: Compilation of Henry's Law Constants for Inorganic and Organic Species of
18 Potential Importance in Environmental Chemistry,, 1999.
- 19 Semiletov, I. P.: Aquatic Sources and Sinks of CO₂ and CH₄ in the Polar Regions, *Journal of*
20 *the Atmospheric Sciences*, 56(2), 286-306, 1999.
- 21 Sonesson, M., Jonsson, S., Rosswall, T. and Rydén, B. E.: The Swedish IBP/PT Tundra
22 Biome Project Objectives-Planning-Site, *Ecological Bulletins*, (30), 7-25, 1980.
- 23 Stumm, W. and Morgan, J. J.: *Aquatic Chemistry: Chemical Equilibria and Rates in Natural*
24 *Waters*, 3rd Edition, Wiley-Interscience., 1996.
- 25 Svensson, B. H., Christensen, T. R., Johansson, E. and Å–quist, M.: Interdecadal Changes in
26 CO₂ and CH₄ Fluxes of a Subarctic Mire: Stordalen Revisited after 20 Years, *Oikos*, 85(1),
27 22-30, 1999.
- 28 Walter, K. M., Chanton, J. P., Chapin, F. S., Schuur, E. A. G. and Zimov, S. A.: Methane
29 production and bubble emissions from arctic lakes: Isotopic implications for source pathways
30 and ages, *J. Geophys. Res.*, 113(G3), G00A08, 2008.

1 Walter, K. M., Smith, L. C. and Stuart Chapin, F.: Methane bubbling from northern lakes:
2 present and future contributions to the global methane budget, *Philosophical Transactions of*
3 *the Royal Society A: Mathematical, Physical and Engineering Sciences*, 365(1856), 1657 -
4 1676, 2007.

5 Walter, K. M., Vas, D. A., Brosius, L., Chapin III, F. S., Zimov, S. A. and Zhuang, Q.:
6 Estimating methane emissions from northern lakes using ice-bubble surveys, *Limnology and*
7 *Oceanography: Methods*, 8, 592-609, 2010.

8 Walter, K. M., Zimov, S. A., Chanton, J. P., Verbyla, D. and Chapin, F. S.: Methane bubbling
9 from Siberian thaw lakes as a positive feedback to climate warming, *Nature*, 443(7107), 71-
10 75, doi:10.1038/nature05040, 2006.

11 Zimov, S. A., Voropaev, Y. V., Davidov, S. P., Zimova, G. M., Davidova, A. I., Chapin III, F.
12 S. and Chapin, M. C.: Flux of methane from North Siberian aquatic systems: Influence on
13 atmospheric methane, in *Permafrost response on economic development, environmental*
14 *security and natural resources*, pp. 511-524, R. Paepe and V. Melnikov., 2001.

1 Table 1. Bounds for methane fluxes released by the winter lake ice cover. The median value is
 2 used if the mean value is higher than the standard deviation.

Methane fluxes (mg CH ₄ m ⁻² d ⁻¹)	Minimum	Mean or median	Maximum
Lake 1	1.34 10 ⁻³	3.01	12.7
Lake 2	3.91 10 ⁻⁴	4.32 10 ⁻²	4.4
Lake 3	6.52 10 ⁻⁵	4.35 10 ⁻⁴	1.14 10 ⁻²
Lake 4	3.59 10 ⁻⁴	3.21 10 ⁻²	4.22

3

4

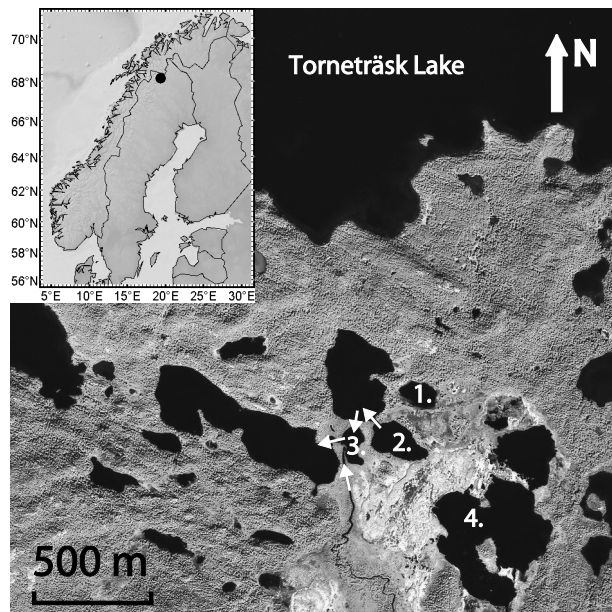


Figure 1. Location map and lakes configuration (the arrows show water connections). The lakes are all embedded in a mire. Lake 1, small and closed; Lake 2, small and connected to another lake; Lake 3, small, receiving water from a river to the South, connected to another lake to the North and draining into another lake to the West; Lake 4, bigger and closed.

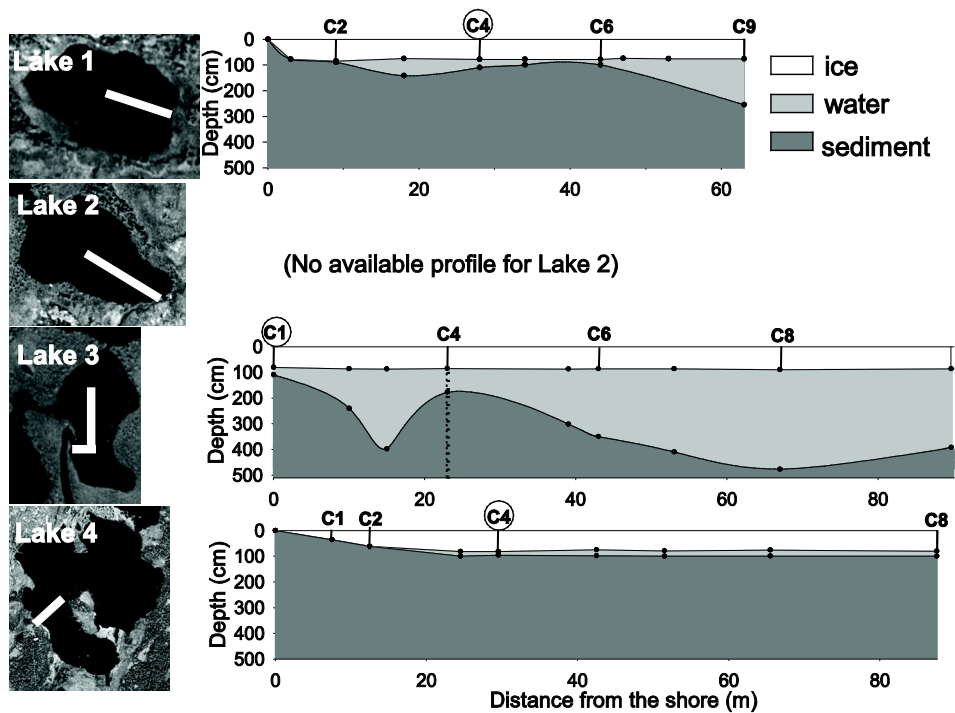


Figure 2. Lakes geometry along the profiles and ice core sampling locations. The white line on lakes shows the transect direction, letters and numbers correspond to the cores studied for the bubbles morphology and circles indicate cores analyzed for their gas properties. The dotted line in the Lake 3 profile shows the change of azimuth of the transect.

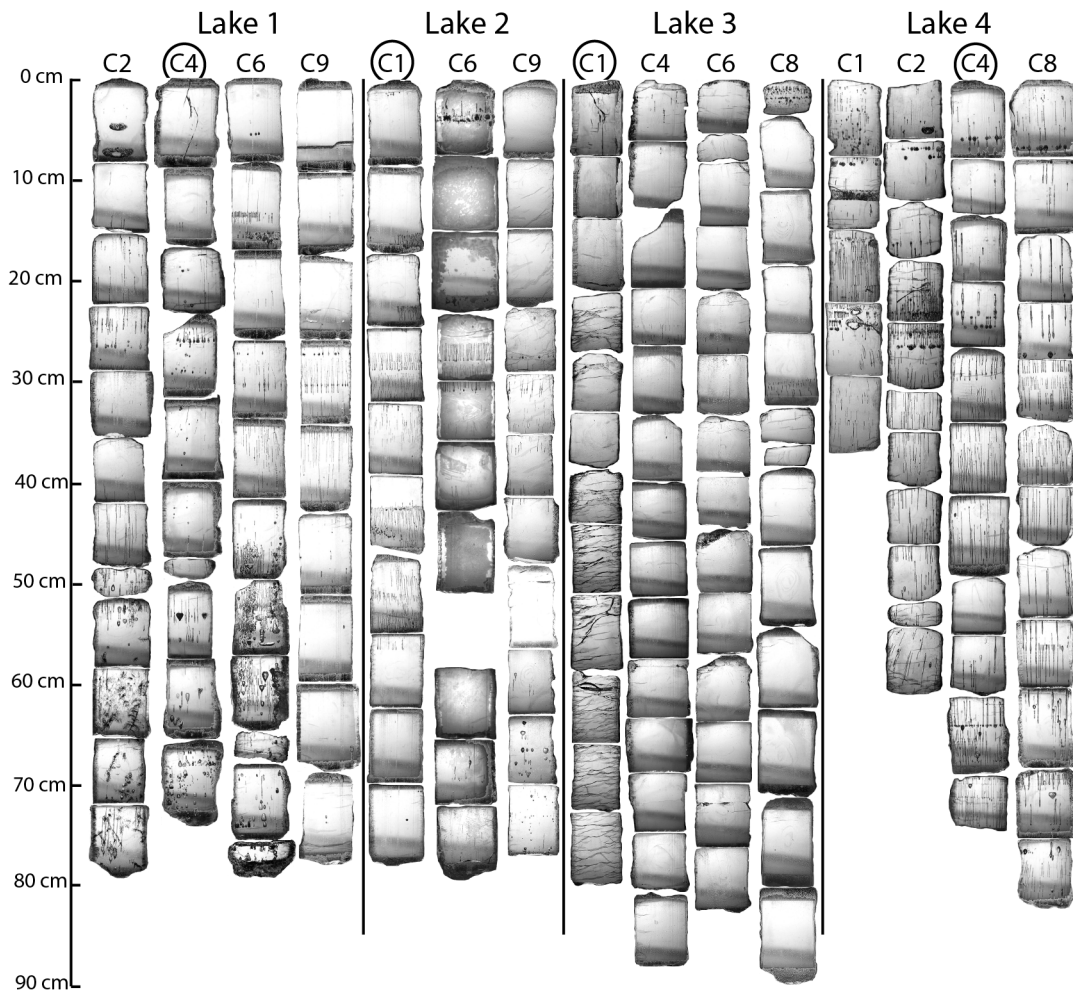


Figure 3. Ice characteristics, bubbles shapes and ~~dispersion~~-distribution in the 15 studied ice cores (see Figure 2 for location). Circles denote the cores analyzed at high resolution for their gas properties.

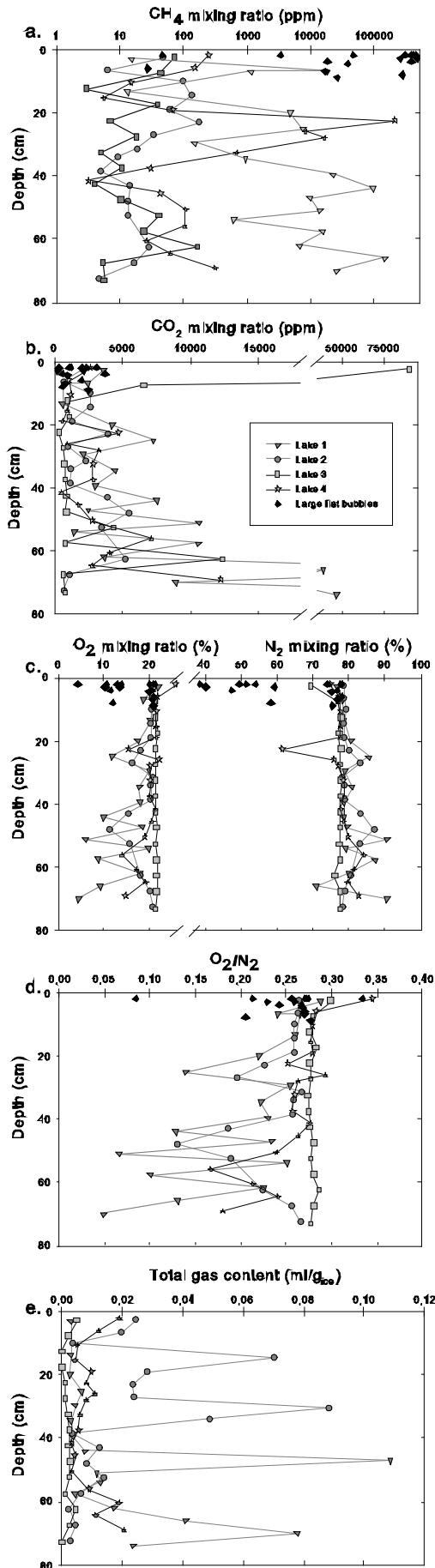


Figure 4. Gas composition and total gas content versus depth for one core of each of the four studied lakes and for fifteen isolated bubbles sampled near the ice surface. A logarithmic scale has been chosen for CH₄. Note that the total gas content is not presented for the isolated bubbles (see text for details).

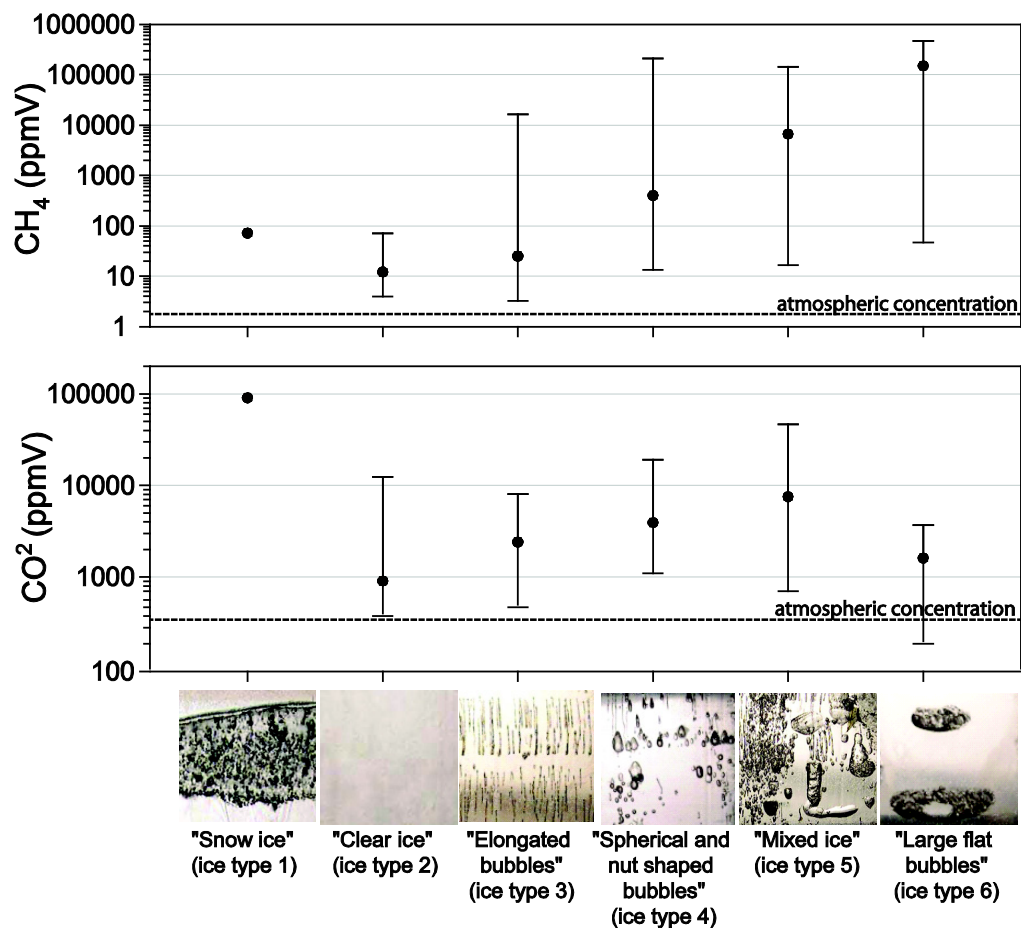


Figure 5. Ice types classification from bubble shapes and density, with associated ranges of CO₂ and CH₄ mixing ratios. Note the logarithmic mixing ratio scale. Black dots are median values and vertical bars represents the variability in the observations.

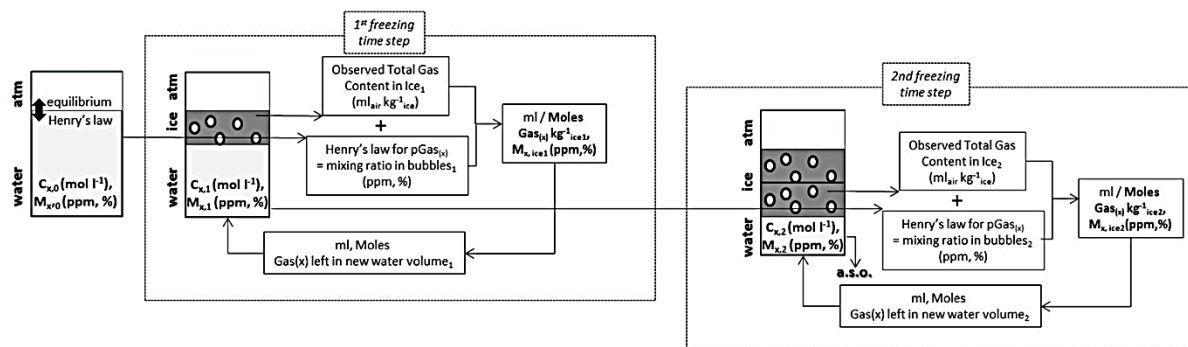
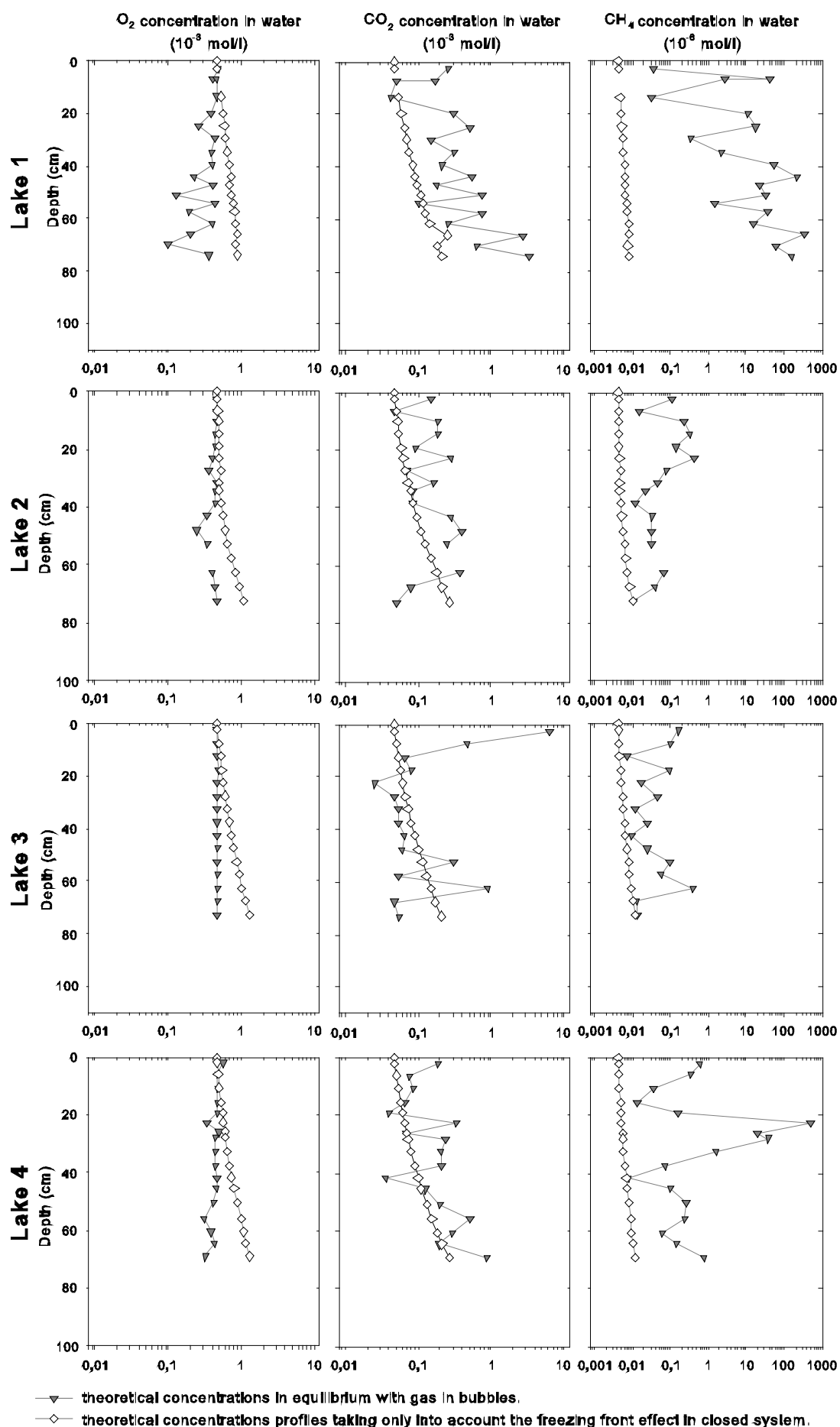


Figure 6: Conceptual diagram for the calculations performed to reconstruct theoretical gas concentrations and mixing ratios in ice and water in the case of a closed system reservoir in which gases are considered as passive tracers (no biogeochemical transformations). C = concentration in water, M = mixing ratio in the water, 0 = initial water, 1 = 1st freezing step, 2 = 2nd freezing step, a.s.o. = repetition of the process. Specific calculation in the case of carbon dioxide, taking into account the carbonate system equilibria, are detailed in the text.



1

Figure 76. Theoretical O_2 , CO_2 and CH_4 concentrations in water as a function of depth for each lake: ~~gray~~ triangles ~~“down”~~ represent values in equilibrium with measured gas mixing ratios in bubbles (calculated using Henry’s law); ~~gray~~ diamonds show **theoretical** values calculated by only taking into account the “reservoir effect” in a closed system (see text for details).

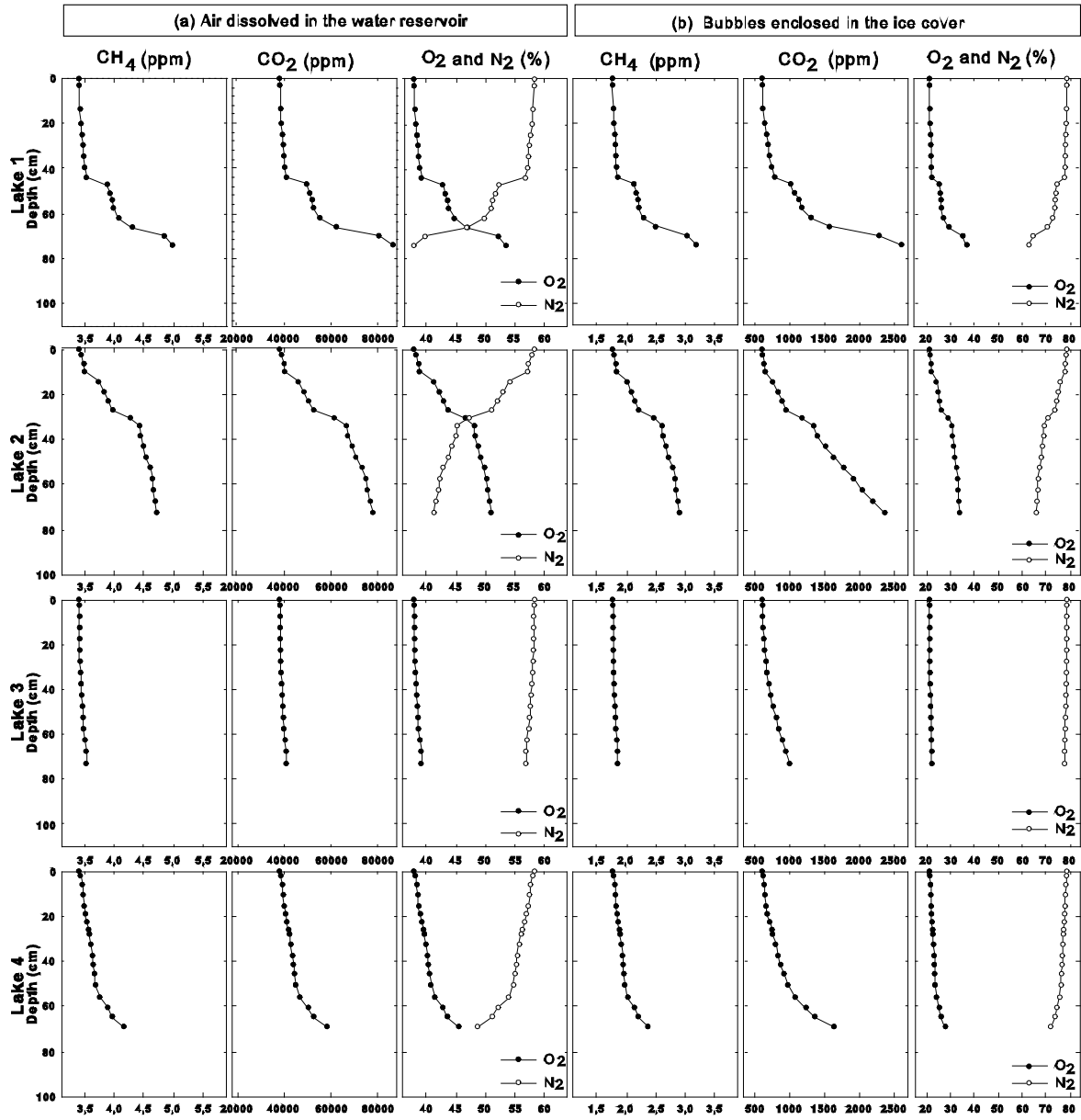


Figure 87. Theoretical evolution of mixing ratios for (a) air dissolved in water and (b) bubbles in ice, assuming lakes are closed reservoir, using observed total gas contents and equilibrium mixing in water from Henry's law for mass balance in the ice and assuming no gas fractionation occurs at the ice water interface (see text for details).

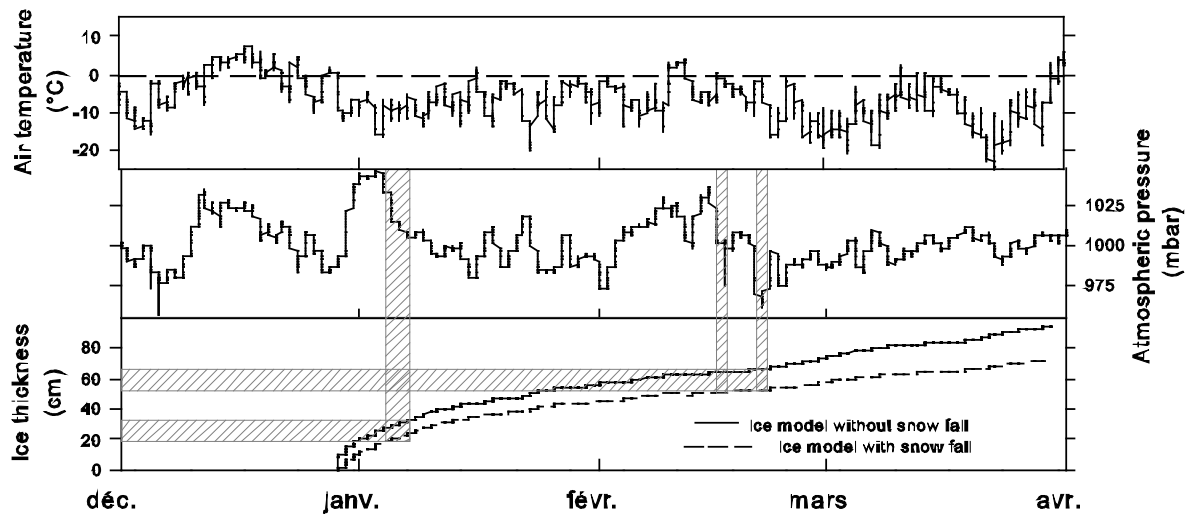


Figure 98. Air temperature and atmospheric pressure versus modeled ice thickness from equation 2 (see text). The dotted line takes snow falls into account. Shadow hatchings show depth fitting with the air pressure drop events. The two highlighted drops correspond with the depth of the two synchronous bubbling events described in the text.